Helmholtz-Zentrum Dresden-Rossendorf (HZDR)

HZDR
HELMHOLTZ ZENTRUM
DRESDEN ROSSENDORF

p-type co-doping effect of (Ga,Mn)P: Magnetic and magneto-transport properties

Xu, C.; Yuan, Y.; Wang, M.; Hentschel, H.; Böttger, R.; Helm, M.; Zhou, S.;

Originally published:

August 2018

Journal of Magnetism and Magnetic Materials 459(2018), 102-105

DOI: https://doi.org/10.1016/j.jmmm.2017.11.124

Perma-Link to Publication Repository of HZDR:

https://www.hzdr.de/publications/Publ-26895

Release of the secondary publication
on the basis of the German Copyright Law § 38 Section 4.

CC BY-NC-ND

P-type co-doping effect of (Ga,Mn)P: Magnetic and magneto-transport properties

Chi Xu[a,b,*], Ye Yuan[a,b], Mao Wang[a,b], Hendrik Hentschel[a,b],

Roman Böttger[a], M. Helm[a,b], Shengqiang Zhou[a]

[a] Helmholtz-Zentrum Dresden Rossendorf, Institute of Ion Beam Physics and Materials Research, Bautzner Landstrasse 400, D-01328 Dresden, Germany

[b] Technische Universität Dresden, D-01062 Dresden, Germany

Abstract

In this paper, we perform a comparison of magnetic and electrical properties between Mn-doped and (Mn, Zn) co-doped GaP dilute ferromagnetic semiconductors. Due to the shallow Zn impurity level (~20-40 meV above the top of the III-V compounds valence band), the Zn co-doping leads to the increase of conductivity of (Ga,Mn)P, however both the Curie temperature and magnetization reduce, which is probably due to the suppression of active Mn substitution by Zn co-doping.

Keywords: dilute ferromagnetic semiconductors; the Curie temperature; magnetization; co-doping; magneto-transport.

[*] Corresponding author.
E-mail address: c.xu@hzdr.de

1. Introduction

Diluted ferromagnetic semiconductors (DFSs) are materials with a combination of magnetic and semiconducting properties, in which ferromagnetism is mediated by holes through *p-d* coupling [1-5]. According to the *p-d* Zener model [2], the Curie temperature (T_C) scales linearly with $p^{1/3}$, where p is the hole concentration. Thus in the past several years, modifying the ferromagnetic behavior through intentionally raising hole concentration attracted a lot of attention [5-8]. One representative example was given by Sawicki et al. [7] via the bias voltage gating on (Ga,Mn)As based semiconductor-insulator-metal structures, and the authors successfully modified both Curie temperature (T_C) and magnetization at the insulator-metal transition regime. In addition, *p*-type nitrogen doping has rendered a ferromagnetic Curie temperature of 1.5 K in spin-glass-like (Zn,Mn)Te [9], proving the validity of modifying ferromagnetic properties by acceptor doping.

Unlike the most studied III-V based DFS (Ga,Mn)As, (Ga,Mn)P has not been under intensive investigation due to its challenging preparation until Scarpulla et al. firstly achieved highly epitaxial (Ga,Mn)P by ion implantation combined with pulsed laser melting [10-12]. However, the experimentally obtained T_C of 65 K is below the Zener-model predicted value of around 100 K when the Mn concentration is around 5%. One reason is that different from (Ga,Mn)As, a stronger *p-d* hybridization between local Mn moments and holes in (Ga,Mn)P induces an deep impurity acceptor level of 440 meV above the top of the valence band [1], preventing metallic behavior with an approachable Mn doping concentration. Therefore, it is of great meaning to tune (Ga,Mn)P magnetic and electrical properties by increasing hole concentration till the sample enters the metallic regime by doping extra acceptors.

In this paper, we intentionally increase the hole concentration in (Ga,Mn)P by doping shallow level acceptor Zn, and investigate the magnetic and electrical properties by comparison of (Ga,Mn)P and Zn co-doped (Ga,Mn)P samples. The extra *p*-type doping leads to an increase of the sample conductivity. However, both T_C and magnetization decrease after Zn-doping. Moreover, the temperature dependent MR behavior changes from the case that a maximal value appears at around T_C in

(Ga,Mn)P to the case that the MR monotonically decreases upon increasing temperature in Zn doped (Ga,Mn)P sample.

2. Material and methods

The Mn and Zn doped, as well as co-doped GaP epilayers were prepared by ion implantation combined with pulsed laser melting. Intrinsic GaP (001) samples were implanted with 80 keV Mn ions with fluence of 1×10^{16} /cm^2 at room temperature. To investigate the co-doping effect, one as-implanted sample and one GaP reference wafer were implanted with Zn by a fluence of 5×10^{15} /cm^2. The implantation energy of Zn was set as 100 keV to obtain a similar ion penetration depth for Zn and Mn in GaP [13]. According to the Stopping and Range of Ions in Matter (SRIM) simulation, the longitudinal straggling (ΔR_P) for the Mn and Zn distribution in GaP is around 50 nm, indicating that the thickness of doping layer is calculated to be 100 nm by $2\Delta R_P$. After implantation, the samples were molten by a pulsed XeCl excimer laser (Coherent COMPexPRO201, λ=308 nm, pulse duration of 30 ns). The energy density of 0.45 J/cm^2 was selected to optimize the crystallization to obtain the highest T_C. After laser treatment, a non-magnetic Mn-rich oxide layer can be generated on the surface [10], preventing the signal of (Ga,Mn)P during the electrical transport measurement. Thus, all samples were immersed in a (1:10) HCl solution at room temperature for 1 hour to etch the oxide layer. A SQUID-VSM (Superconducting Quantum Interference Device - Vibrating Sample Magnetometer) was used to measure magnetic properties of all samples. The magneto-transport measurements were performed by using a Lake Shore Hall Measurement System in the van der Pauw geometry. The Mn and Zn concentrations are determined by particle induced X-ray emission (PIXE).

3. Results and discussion

Table 1 The Mn and Zn concentrations measured by PIXE (error<4%), Curie temperatures determined by SQUID-VSM and activation energies calculated by Eq (1) of all samples.

Sample No.	Mn Conc. (%)	Zn Conc. (%)	T_C (K)	E (meV)
sample A	1.3	-	35	23

sample B	1.3	0.9	20	8
sample C	-	0.9	-	-

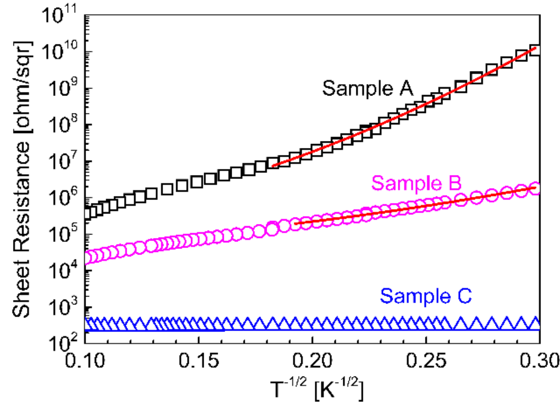

Fig. 1. Sheet resistance versus $T^{-1/2}$ under zero field of samples A (squares), B (circles), and C (triangles).

To investigate the electrical transport properties, the temperature-dependent sheet resistance of sample A, B and C are present in Fig. 1. For the reference sample C, the sheet resistance increases with increasing temperature, indicating a metallic characteristic. This phenomenon indicates that the doped Zn concentration is sufficient to render the Fermi level to enter the GaP valence band. An insulating characteristic is observed in the sample doped with only Mn. Moreover, a linear dependence of sheet resistance vs $T^{-1/2}$ at the temperature regime below T_C indicates that the variable range hopping conduction is mainly in charge of the electrical transport [14]. To describe the mentioned conduction process [10], a hopping conduction model is given in Eq. (1):

$$\rho = \rho_0 exp\left(\frac{E}{k_B T}\right)^{\frac{1}{2}} \quad (1)$$

where the pre-exponential constant ρ_0 and activation energy E are the free parameters. For sample A with Mn concentration of 1%, an activation energy of ~23 meV at low temperature regime is calculated. This value is larger than the one in (In,Mn)P [15], due to the deeper Mn impurity level in (Ga,Mn)P (400 meV above the valence band top) than in (In,Mn)P (220 meV above the valence band top). It is worth noting that the Mn and Zn co-doped sample still shows an insulating feature even its conductivity is four orders larger than (Ga,Mn)P. It suggests that the Fermi level goes back to the

gap due to the strong *p-d* hybridization between Mn *3d* orbital and holes residing in the phosphorus *p*-orbital. We note that the linear dependence of sheet resistance vs $T^{-1/2}$ below T_C presents a variable range hopping conducting characteristic, and the hopping energy in sample B reduces to 8 meV, proving that the distance between the valence band top and the isolated Mn impurity band shrinks by the emerging of the Zn impurity level with the GaP valence band.

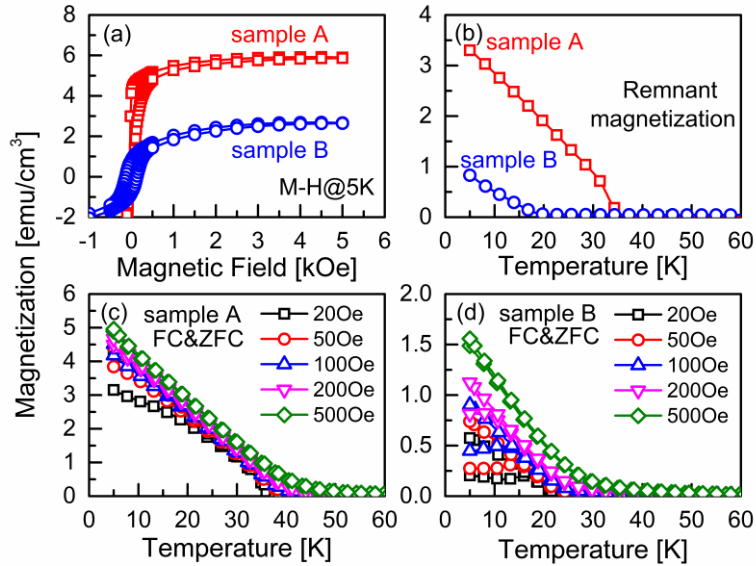

Fig. 2. Magnetic field dependent magnetization at 5 K (a) and thermo-remnant magnetization (b) of sample A (open squares) and sample B (open cycles). Temperature dependent field cooling down and zero field cooling down procedure of sample A (c) and sample B (d).

Magnetic field dependent hysteresis loops and temperature dependent magnetization of samples A and B are shown in Fig. 2. The appearance of hysteresis loops in both samples A and B indicates the exhibiting of ferromagnetic coupling. For sample A, the remnant magnetization versus temperature curve in Fig. 2b indicates that the Curie temperature is around 35 K where the magnetization vanishes. In addition, the overlapping of temperature-dependent field cooling (FC) and zero field cooling (ZFC) measurement curves of sample A confirms the global ferromagnetic nature, as displayed in Fig. 2c. However, both saturation magnetization and remnant magnetization decrease in co-doped sample B when compared to sample A at 5 K. Moreover, the temperature dependent remnant magnetization presents that the zinc doping causes a reduction of T_C from 35 to 20 K. Both of above two phenomena

suggest the decreasing of active substitutional Mn atom concentration. According to the FC-ZFC measurement results shown in Fig. 2d, a sign of superparamagnetic behavior is observed: A bifurcation is present between the ZFC and FC curves where a maximum (average blocking temperature T_B) shows up in the ZFC process. Moreover, the T_B shifts to the low temperature side upon increasing applied fields. According to a study of GaMnAs, the decreased Mn concentration causes appearance of superparamagnetic phase [16], which is quite similar with GaMnP. Interestingly, according to the PIXE results of samples A and B, the Zn doping does not result in the reduction of Mn content in the layer. Thus, the reason of decreased magnetization and T_C can be explained by two possibilities: (1) Parts of substitutional Mn atoms are placed on the interstitial sites to energetically stabilize the whole system by compensating holes [1]. (2) The formation of Mn-Zn dimer reduces the active Mn atom density to lower the system energy. This phenomenon was observed in Mg doped (Ga,Mn)N [17].

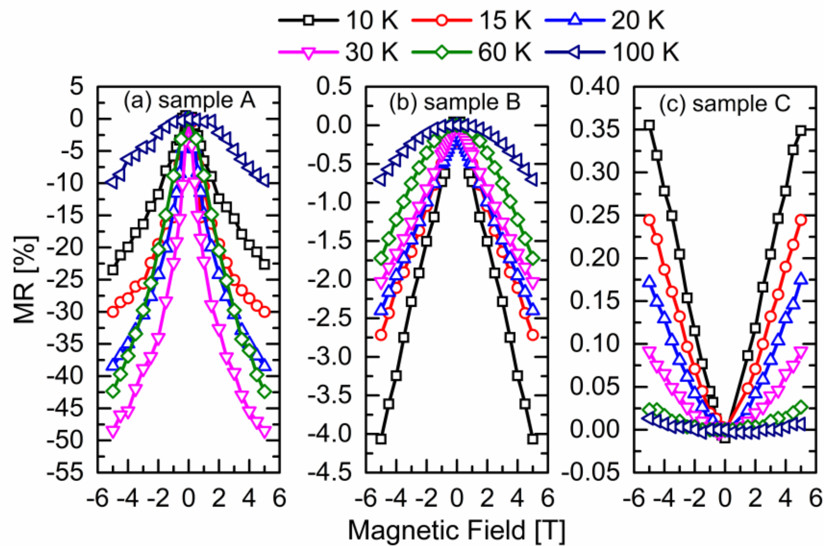

Fig. 3. Magnetic field dependent magnetoresistance of samples A (a), B (b), and C (c) at temperatures of 10, 15, 20, 30, 60 and 100 K.

Fig. 3 shows the magnetic field dependent magnetoresistance (MR) of all samples measured at temperatures of 10, 15, 20, 30, 60, and 100 K, where MR is defined as $\frac{\rho(H)-\rho(0)}{\rho(0)} \times 100\%$. A negative MR is defined by the reduced resistance upon increasing magnetic field in both samples A and B. The negative MR results from the

reduction of scattering between spin polarized holes and Mn local moments when an external magnetic field is applied. This is an immediate consequence of the antiferromagnetic coupling between the hole and the Mn local moment. Interestingly, the negative MR does not show any saturation signature even at a field of 5 T, where the ferromagnetism has been saturated as shown in Fig. 2 (a) and (b). This unsaturated negative MR can be explained either by the scattering from the spin polarized holes and unsaturated paramagnetic Mn [18] or by the quantum localization effect [19]. For sample A, the maximal MR is as large as 48% which is larger than the 16% in sample B when a 5 T field is applied. Expectedly, only a positive MR is seen in the Zn doped sample C, and the maximal value is 0.35% at 10 K, which can be explained by the decreased carrier mobility under a magnetic field, i.e. the ordinary magnetoresistance [20]. As shown in Fig. 4, we note that the maximal negative MR appears at T_C in sample A. The maximal negative MR at T_C can be interpreted as critical scattering by packets of the magnetic spins with a ferromagnetic short-range order characterized by the correlation length comparable to the wavelength of the carriers at the Fermi level. The same phenomenon was observed in metallic (Ga,Mn)As [21]. Different from sample A, the maximal negative MR value appears at the lowest measured temperature in sample B. Moreover, the negative MR monotonically decreases upon increasing temperature as shown in Fig. 4.

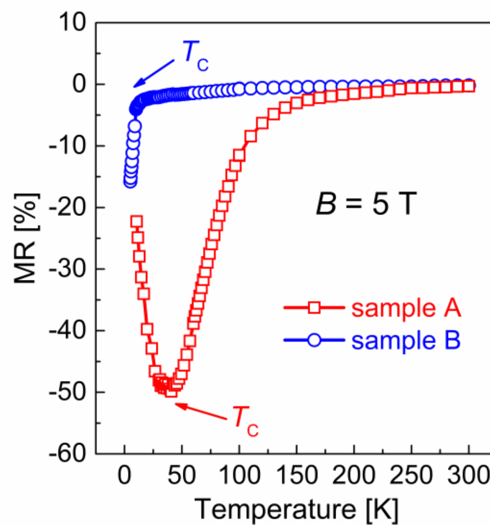

Fig. 4. Temperature dependent magneto-resistance at 5 T of samples A and B.

4. Conclusion

We have investigated the magnetic and electrical properties of (Ga,Mn)P and Zn doped (Ga,Mn)P samples. The conductivity is enlarged by zinc doping. After Zn doping, in addition to the decreased Curie temperature and magnetization, the blocking superparamagnetic behavior instead of ferromagnetic coupling is present, probably due to the suppression of the active substitutional Mn atoms. In addition, the temperature dependence of the negative MR is also changed from persisting a peak value at around T_C in (Ga,Mn)P to temperature monotonic decreasing in (Ga,Mn)P:Zn.

Acknowledgments

Support by the Ion Beam Center (IBC) at HZDR is gratefully acknowledged. This work is funded by the Helmholtz-Gemeinschaft Deutscher Forschungszentren (HGF-VH-NG-713). The author C. X. thanks financial support by Chinese Scholarship Council (File No. 201306120027).

References

[1] T. Dietl, H. Ohno, Dilute ferromagnetic semiconductors: Physics and spintronic structures, Rev. Mod. Phys., 86 (2014) 187-251.
[2] T. Dietl, H. Ohno, F. Matsukura, J. Cibert, D. Ferrand, Zener model description of ferromagnetism in zinc-blende magnetic semiconductors, Science, 287 (2000) 1019-1022.
[3] D. Chiba, M. Sawicki, Y. Nishitani, Y. Nakatani, F. Matsukura, H. Ohno, Magnetization vector manipulation by electric fields, Nature, 455 (2008) 515-518.
[4] H. Ohno, Making nonmagnetic semiconductors ferromagnetic, Science, 281 (1998) 951-956.
[5] H. Ohno, D. Chiba, F. Matsukura, T. Omiya, E. Abe, T. Dietl, Y. Ohno, K. Ohtani, Electric-field control of ferromagnetism, Nature, 408 (2000) 944-946.
[6] T. Dietl, H. Ohno, F. Matsukura, Hole-mediated ferromagnetism in tetrahedrally coordinated semiconductors, Phys. Rev. B, 63 (2001) 195205.
[7] M. Sawicki, D. Chiba, A. Korbecka, Y. Nishitani, J.A. Majewski, F. Matsukura, T. Dietl, H. Ohno, Experimental probing of the interplay between ferromagnetism and localization in (Ga, Mn)As, Nat. Phys., 6 (2009) 22-25.
[8] S.-y. Koshihara, A. Oiwa, M. Hirasawa, S. Katsumoto, Y. Iye, C. Urano, H. Takagi, H. Munekata, Ferromagnetic order induced by photogenerated carriers in magnetic III-V semiconductor heterostructures of (In, Mn) As/GaSb, Phys. Rev. Lett., 78 (1997) 4617.
[9] D. Ferrand, J. Cibert, C. Bourgognon, S. Tatarenko, A. Wasiela, G. Fishman, A. Bonanni, H. Sitter, S. Kolesnik, J. Jaroszyski, A. Barcz, T. Dietl, Carrier-induced ferromagnetic interactions in p-doped $Zn_{1-x}Mn_xTe$ epilayers, J. Cryst. Growth, 214 (2000) 387-390.
[10] M.A. Scarpulla, B.L. Cardozo, R. Farshchi, W.M. Oo, M.D. McCluskey, K.M. Yu, O.D. Dubon,

Ferromagnetism in Ga(1-x)Mn(x)P: evidence for inter-Mn exchange mediated by localized holes within a detached impurity band, Phys. Rev. Lett., 95 (2005) 207204.
[11] Y. Yuan, Y. Wang, M. Khalid, K. Gao, S. Prucnal, O.D. Gordan, G. Salvan, D.R.T. Zahn, W. Skorupa, M. Helm, S. Zhou, Ferromagnetic GaMnP Prepared by Ion Implantation and Pulsed Laser Annealing, IEEE Trans. Magn., 50 (2014) 1-4.
[12] Y. Yuan, R. Hubner, F. Liu, M. Sawicki, O. Gordan, G. Salvan, D.R. Zahn, D. Banerjee, C. Baehtz, M. Helm, S. Zhou, Ferromagnetic Mn-Implanted GaP: Microstructures vs Magnetic Properties, ACS Appl Mater Interfaces, 8 (2016) 3912-3918.
[13] D. Bürger, S. Zhou, J. Grenzer, H. Reuther, W. Anwand, V. Gottschalch, M. Helm, H. Schmidt, The influence of annealing on manganese implanted GaAs films, Nucl. Instrum. Meth. B, 267 (2009) 1626-1629.
[14] A. Kaminski, S.D. Sarma, Magnetic and transport percolation in diluted magnetic semiconductors, Phys. Rev. B, 68 (2003) 235210.
[15] M. Khalid, E. Weschke, W. Skorupa, M. Helm, S. Zhou, Ferromagnetism and impurity band in a magnetic semiconductor: InMnP, Phys. Rev. B, 89 (2014) 121301.
[16] Y. Yuan, C. Xu, R. Hübner, R. Jakiela, R. Böttger, M. Helm, M. Sawicki, T. Dietl, S. Zhou, Interplay between localization and magnetism in (Ga,Mn)As and (In,Mn)As, Phys. Rev. Mater., 1 (2017) 054401.
[17] T. Devillers, M. Rovezzi, N.G. Szwacki, S. Dobkowska, W. Stefanowicz, D. Sztenkiel, A. Grois, J. Suffczynski, A. Navarro-Quezada, B. Faina, T. Li, P. Glatzel, F. d'Acapito, R. Jakiela, M. Sawicki, J.A. Majewski, T. Dietl, A. Bonanni, Manipulating Mn-Mgk cation complexes to control the charge- and spin-state of Mn in GaN, Sci Rep, 2 (2012) 722.
[18] M. Csontos, T. Wojtowicz, X. Liu, M. Dobrowolska, B. Janko, J.K. Furdyna, G. Mihaly, Magnetic scattering of spin polarized carriers in (In, Mn)Sb dilute magnetic semiconductor, Phys. Rev. Lett., 95 (2005) 227203.
[19] F. Matsukura, M. Sawicki, T. Dietl, D. Chiba, H. Ohno, Magnetotransport properties of metallic (Ga, Mn) As films with compressive and tensile strain, Physica E: Low-dimensional Systems and Nanostructures, 21 (2004) 1032-1036.
[20] J. Hu, T.F. Rosenbaum, Classical and quantum routes to linear magnetoresistance, Nat Mater, 7 (2008) 697-700.
[21] F. Matsukura, H. Ohno, A. Shen, Y. Sugawara, Transport properties and origin of ferromagnetism in (Ga, Mn) As, Phys. Rev. B, 57 (1998) R2037.